

THE COLLEGE OF AERONAUTICS  
CRANFIELD



AERODYNAMIC CHARACTERISTICS OF A  $40^\circ$   
SWEPT BACK WING OF ASPECT RATIO 4.5

by

P. S. BARNA

MAY, 1957THE COLLEGE OF AERONAUTICSCRANFIELD

A preliminary report on the  
aerodynamic characteristics  
of a  $40^{\circ}$  swept back wing of  
aspect ratio 4.5

- by -

P. S. BARNA, M. E.

SUMMARY

Experimental investigations have been made of the flow characteristics on wings of moderate sweepback. This note presents the results of the experimental investigation into the pressure distribution over a swept back wing, having an aspect ratio 4.5 and sweep back angle  $40^{\circ}$  at quarter chord. A half model technique has been used. The wing section was R. A. E. 101 (symmetrical) with 6% maximum thickness and zero camber. Measurements of chordwise pressure distributions at a number of spanwise sections were made in the incidence range  $2 - 32^{\circ}$ . The experiments were performed at Reynolds numbers of  $0.9 \times 10^6$  and  $2 \times 10^6$  (based on geometric mean chord). From these measurements, lift, drag and pitching moment characteristics of the wing were calculated. Results of the experiments for small incidences have been compared with the calculated loadings

obtained by methods proposed by Kucheman. <sup>(1)</sup> The theory predicts higher values in the spanwise load distribution at the root stations and a lift curve slope 8-12 percent lower than obtained in the experiments.

Prepared under Ministry of Supply Contract No 7/Expt1/629/PR3

### TEST EQUIPMENT

The half wing was mounted in a vertical position on the turntable of the 8' x 6' low speed wind tunnel of the College of Aeronautics(Fig. 1) The tunnel floor represented the wing reflection plane. The relevant dimensions of the wing and the chordwise and the spanwise location of the pressure tapings are shown in Fig. 2. Only one side of the wing was provided with pressure tapping holes. Pressure readings were recorded at the following angles of incidence: 2, 4, 6, 7, 8, 10, 12, 14, 17, 20, 24, 28 and 32<sup>0</sup>.

In order to reduce the floor boundary layer thickness in the root section of the model boundary layer suction was applied by means of a perforated plate set in the floor of the tunnel 5 ft. upstream of the centre of the turntable. The boundary layer air was returned into the tunnel at the inlet to the diffuser following the working section. An axial flow fan running at speeds up to 24, 000 r. p. m. was employed for the removal of the boundary layer. Manometers employed for the pressure measurements were the standard vertical type fitted with the standard clamping device using alcohol as indicator fluid. The air speed in the working section was obtained from the pressure difference between the settling chamber and the calibration static hole in the working section with the aid of a Betz manometer.

### EXPERIMENTAL PROCEDURE

Preliminary tests were made to determine the effect of boundary layer suction on the wing pressure distribution. It was found that although the changes in pressure with change in boundary layer suction were small nevertheless it appeared desirable to employ suction, but that above a certain suction quantity there appeared no further improvement on the pressure distribution. As a result the tests at a Reynolds number of  $0.96 \times 10^6$  were with suction fan running at 24, 000 r. p. m. and the tests at a Reynolds number of  $2 \times 10^6$  were performed with the suction fan running at

15,000 r. p. m.

Since the wing was provided with tapping on one side only it was first set at an incidence  $+\alpha$  thus providing a pressure distribution of the upper surface. The manometers having been read, the wing was set at an incidence  $-\alpha$  thus providing a pressure distribution of the lower surface.

### CALIBRATION OF THE TUNNEL

Prior to the experiments the tunnel was calibrated for flow uniformity and static pressure gradient with different boundary layer suction, the suction fan speed varying from zero to 24,000 r. p. m.

### CALCULATION OF TEST RESULTS

Standard procedure was adopted for the calculations of test results. First, at a given angle of incidence the pressure coefficients defined by  $C_p = \frac{p - p_0}{\frac{1}{2} \rho v^2}$  were plotted for each chordwise section at specified spanwise positions. Values of  $C_p$  were plotted both against  $x/c$  and  $z/c$ . where  $x$  and  $z$  were measured parallel and normal to the wing chord. The local lift and pressure drag values were obtained from graphical integration of the areas under the curves using the relations

$$C_L = A_1 \cos \alpha - A_2 \sin \alpha$$

$$C_D = A_1 \sin \alpha + A_2 \cos \alpha$$

where  $C_L, C_D$  = the local lift and pressure drag coefficients

$$A_1 = \oint C_p \frac{dx}{c} \text{ and } A_2 = \oint C_p \frac{dz}{c}$$

With these values of  $C_L$  and  $C_D$  the product  $C_L c$  and  $C_D c$  was obtained ( $c$  being the local chord) and subsequently the  $C_L c$ ,  $C_D c$  curves were plotted against spanwise location  $\eta$ . Finally, on integration of these areas, the overall lift and pressure drag coefficients were obtained from

$$\bar{C}_L = \frac{1}{\bar{c}} \int_0^1 C_L c \, d\eta$$

$$\bar{C}_D = \frac{1}{\bar{c}} \int_0^1 C_D c \, d\eta$$

where  $\bar{C}$  = geometrical mean chord.

The pitching moment coefficient of the wing about the root leading edge was obtained from

$$\bar{C}_{m \text{ R.L.E.}} = \frac{1}{\bar{c}^2} \int_0^1 C_m(h) c \, d\eta$$

where

$$C_m(h) = C_m(0) - C_N \left( \frac{h+c}{\bar{c}} \right),$$

$h$  being the streamwise distance between leading edge and root leading edge and  $C_m(0)$  = the pitching moment about the local wing leading edge.

## PRESENTATION OF TEST RESULTS

The overall lift and pressure drag coefficients plotted against geometric incidence are shown in Fig. 3, the pitching moment coefficient plotted against lift coefficient in Fig. 4, the distribution of the local lift coefficient in Fig. 5 and the local lift curve slope plotted against spanwise location in Fig. 6. The load distribution along the span is given in Fig. 7 and the spanwise position of aerodynamic centres in Fig. 8.

## BRIEF DISCUSSION OF THE TEST RESULTS.

The overall lift coefficient varies linearly with incidence up to  $6^\circ$  approximately (Fig. 3.), the lift curve slope  $\bar{C}_L / \alpha$  being 3.45. This agrees fairly well with theory<sup>(1)</sup> which gives 3.33 for  $\bar{C}_L / \alpha$ . Above  $6^\circ$  the lift curve slope increases up to  $8^\circ$  then decreases with increasing incidence. Maximum lift is obtained between  $20$ - $22^\circ$  incidence,  $C_{L \text{ max.}}$  being 0.975 and 0.96 for the high and low Reynolds number tests, respectively. Reynolds number effects over the small range of Reynolds numbers tested appear to be small up to  $20^\circ$  incidence, beyond this, however, the effects become noticeable.

It has been shown from a surface flow investigation (details of which will be given in a separate report) that leading edge separation starts at approximately  $6^\circ$  incidence. Hence the deviation of the lift curve from a straight line is consistent with the appearance of the part span vortex. This moves inboard with increasing incidence which greatly affects the spanwise lift distribution. The local  $C_{L \text{ max.}}$  moves inboard as shown in Fig. 5. The highest value of the local lift coefficient is approximately 1.32 and may be observed at  $20^\circ$  incidence at the spanwise station  $\eta = 0.175$ . Flow visualization tests indicate that a part span vortex still exists above  $20^\circ$ . It is shown in Fig. 5 that above  $20^\circ$  incidence the lift gradually decreases at the root although it slightly increases towards the tip.

The distributions of local lift coefficient (Fig. 5) agree fairly well for both the high and low Reynolds numbers cases except for  $10^\circ$  incidence. The latter disagreement may be attributed to inaccuracy of the pressure readings due to marked unsteadiness in the pressure distribution at this incidence.

The pitching moment shows a fairly linear relationship with  $\bar{C}_L$  up to  $\bar{C}_L = 0.75$  (Fig. 4) which corresponds to  $\alpha = 12^\circ$  which is somewhat surprising in view of the development of the



part span vortex about  $6^{\circ}$  incidence. Above this incidence a stable type of stall occurs (nose down moment). The aerodynamic centre is 1.90 ft. from the root leading edge as compared with the theoretical value of 2.02.

The variation of the local lift curve slope (Fig. 6) is in fair agreement with the theory <sup>(1)</sup>, and the difference between the theoretical and experimental values is 8-12%.

The distribution of spanwise loading (Fig. 7) in the incidence range  $2 - 6^{\circ}$  agrees fairly well with the theoretical curve except near the root where the theory predicts higher values than those obtained by experiment. The positions of aerodynamic centres along the span, (Fig. 8) also agree well with theory, the experimental results being somewhat lower than the theoretical values.

#### ACKNOWLEDGEMENTS

The theoretical calculations were performed by Mr P. Sharman. The lower Reynolds number tests were made by Messrs G. Appleby and E. Kendall. The tunnel was operated throughout these tests by Mr S. H. Lilley. Mrs Mc Nally assisted both in taking the readings and reducing the results.

Reference. (1) A simple method of calculating the span and chordwise loading on straight and swept wings. By D. Kucheman. R. A. E. Report Aero 2476.



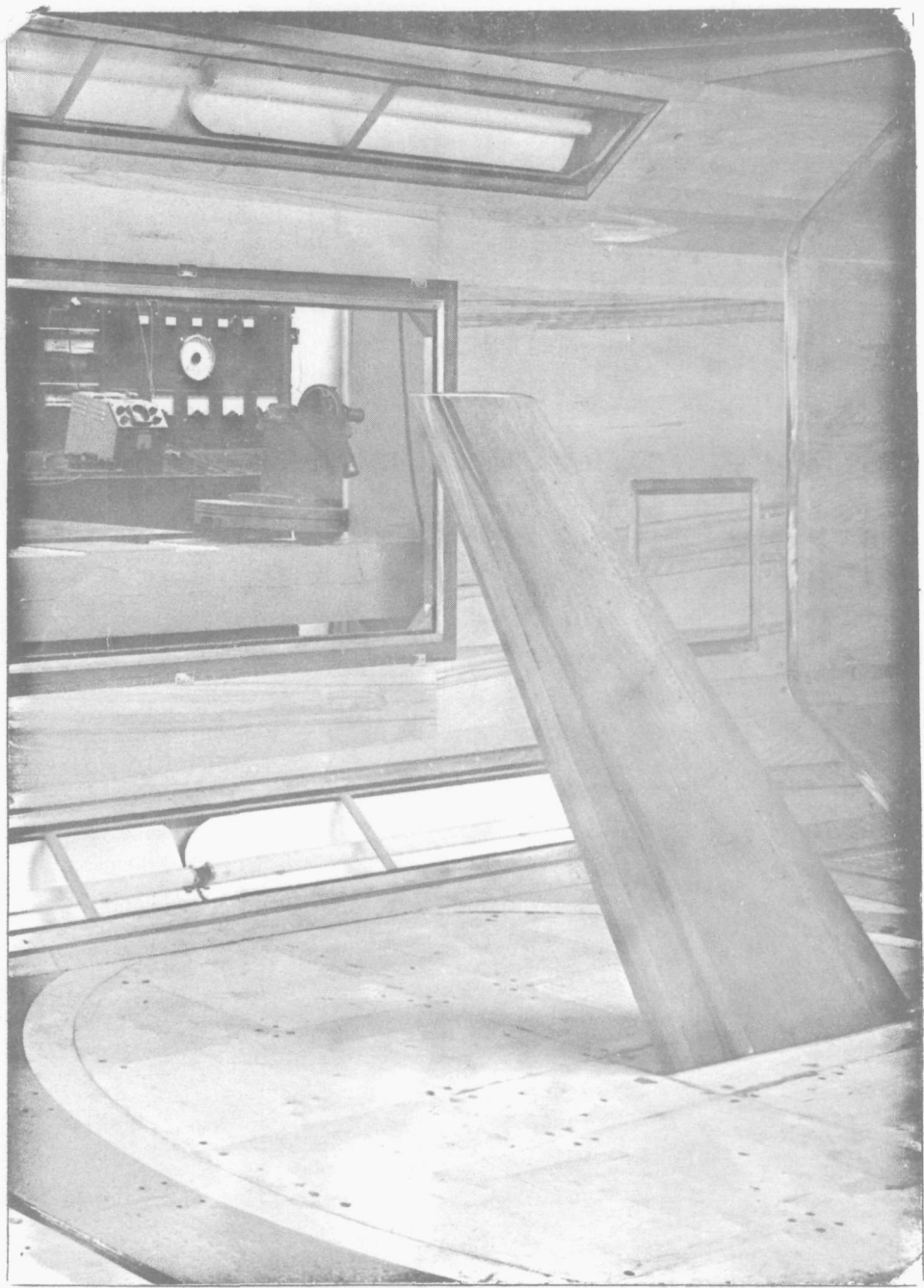
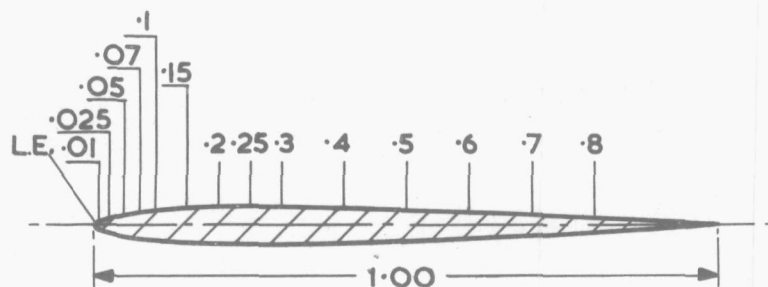


FIG. 1



WING SECTION SHOWING APPROXIMATE LOCATION  
OF PRESSURE HOLES.

WING SECTION R.A.E. 101

MAX.  $t/c = 0.06$  at  $x = 0.3c$

ASPECT RATIO 4.5

TAPER RATIO 0.4

$1/4c$  LINE SWEEPBACK  $40^\circ$

L.E. SWEEPBACK  $43^\circ 3'$

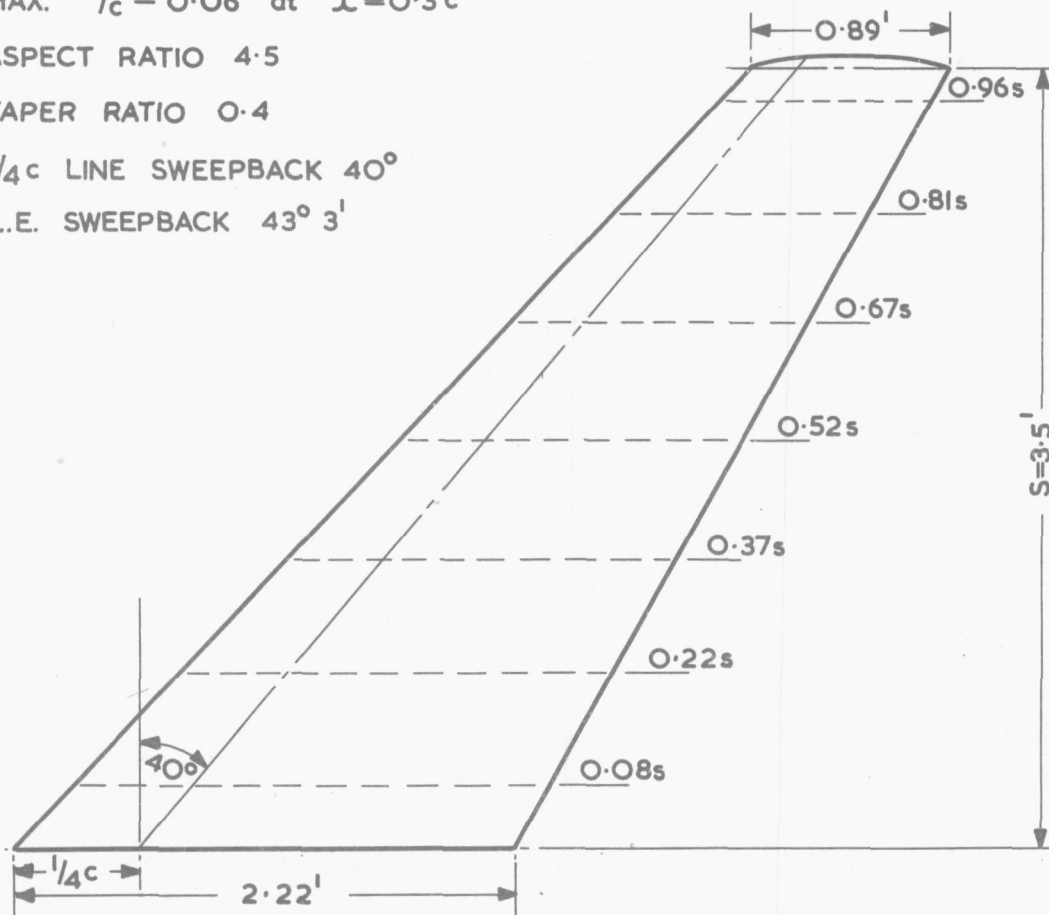


FIG. 2. PLANFORM DIMENSIONS OF WING.

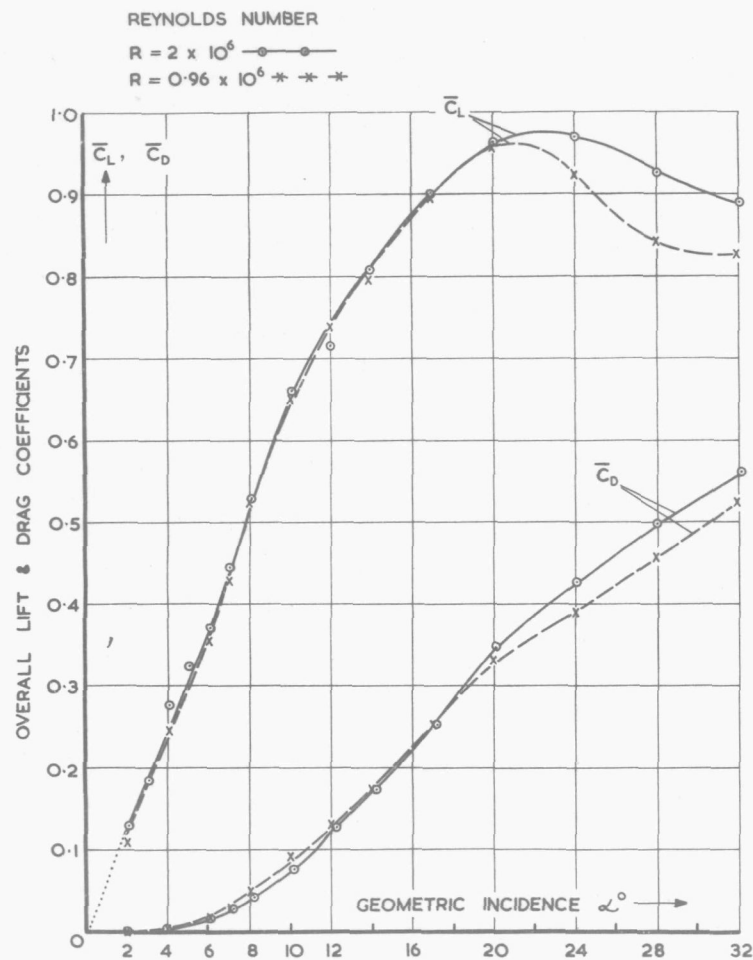


FIG. 3. OVERALL LIFT AND PRESSURE DRAG COEFFICIENT.

AR = 4.5

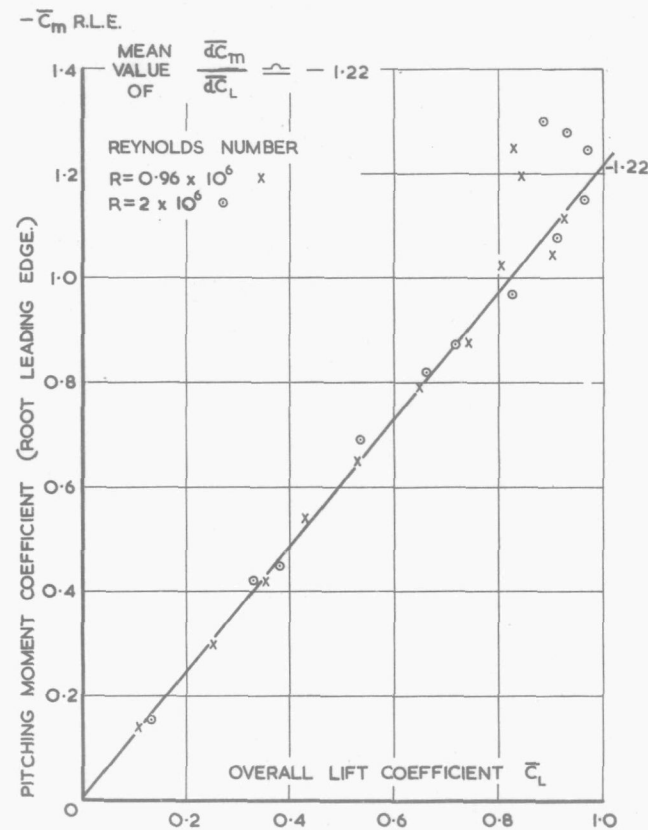


FIG. 4. VARIATION OF OVERALL PITCHING MOMENT WITH OVERALL LIFT COEFFICIENT.

AR = 4.5

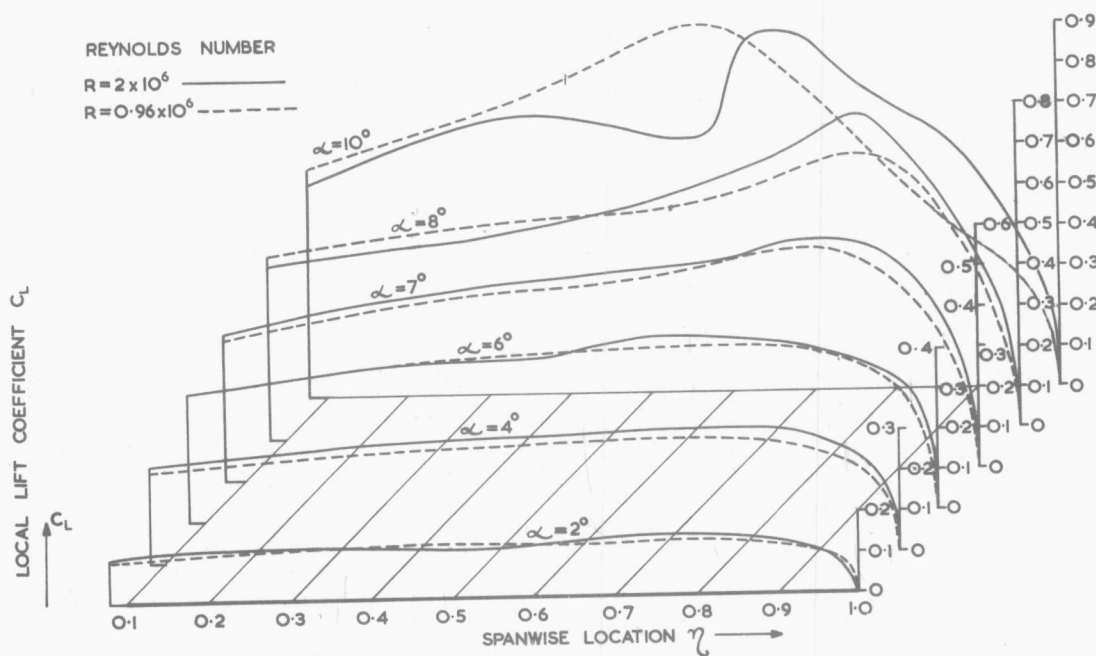
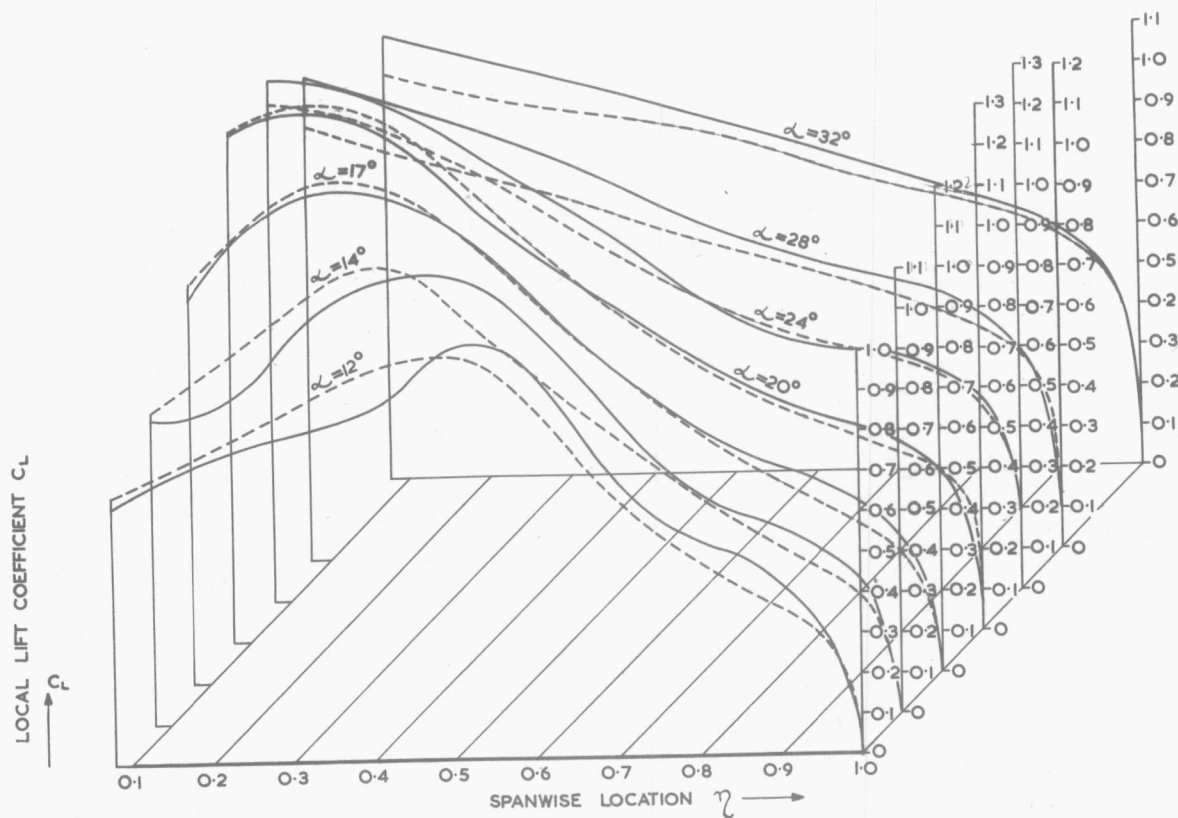


FIG. 5. DISTRIBUTION OF LOCAL LIFT COEFFICIENT  $C_L$  ALONG THE SPAN.  
 $AR=4.5$

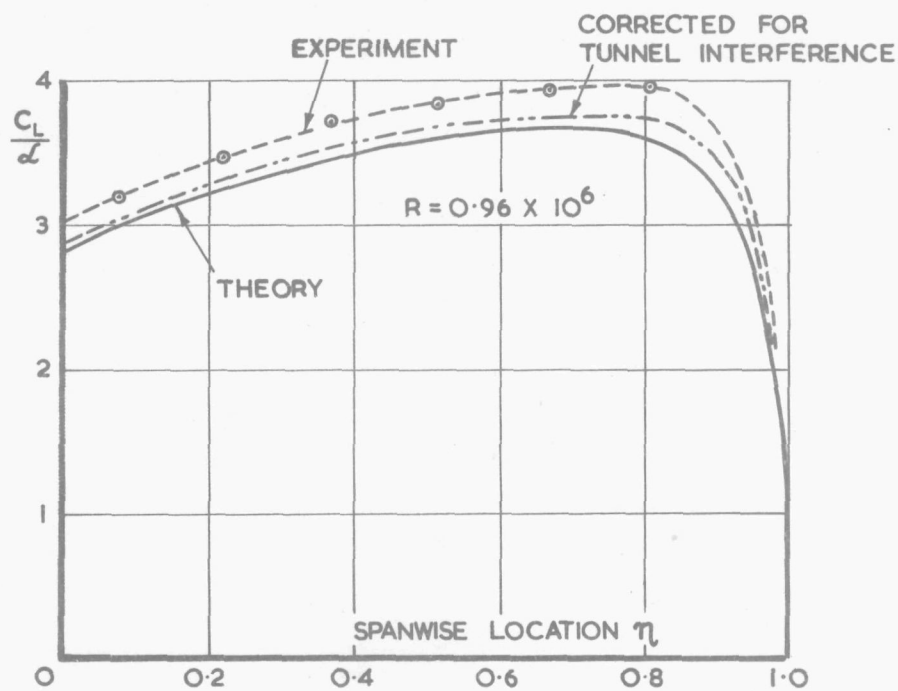
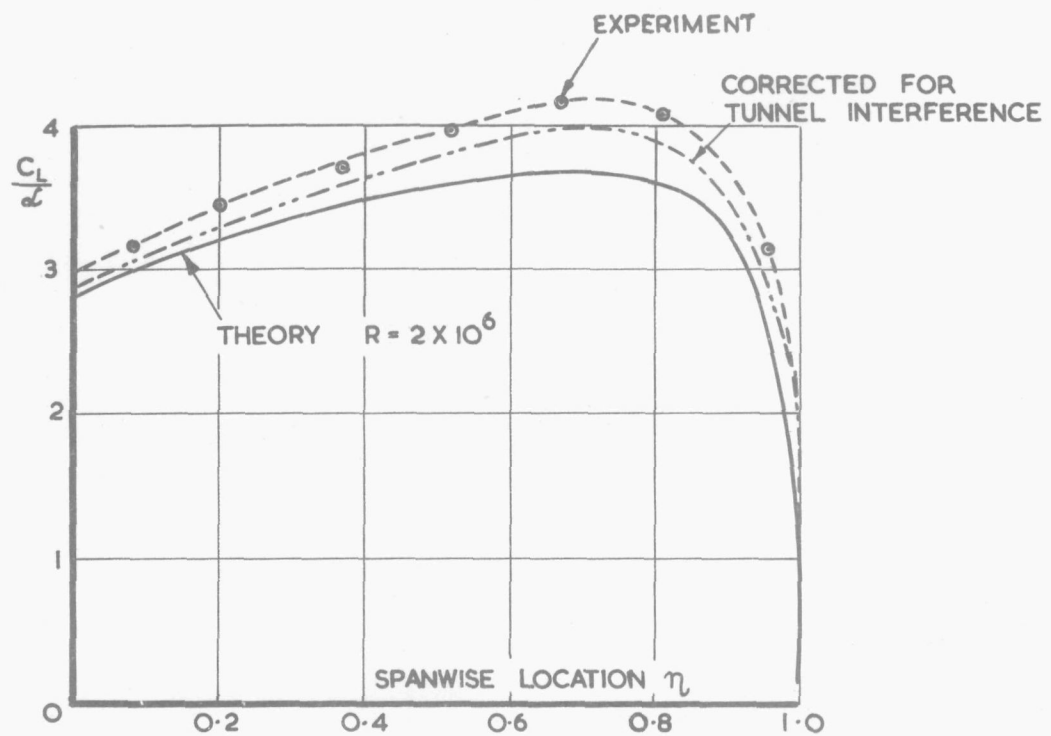


FIG. 6. VARIATION OF LOCAL LIFT CURVE SLOPE ALONG THE SPAN

AR=4.5

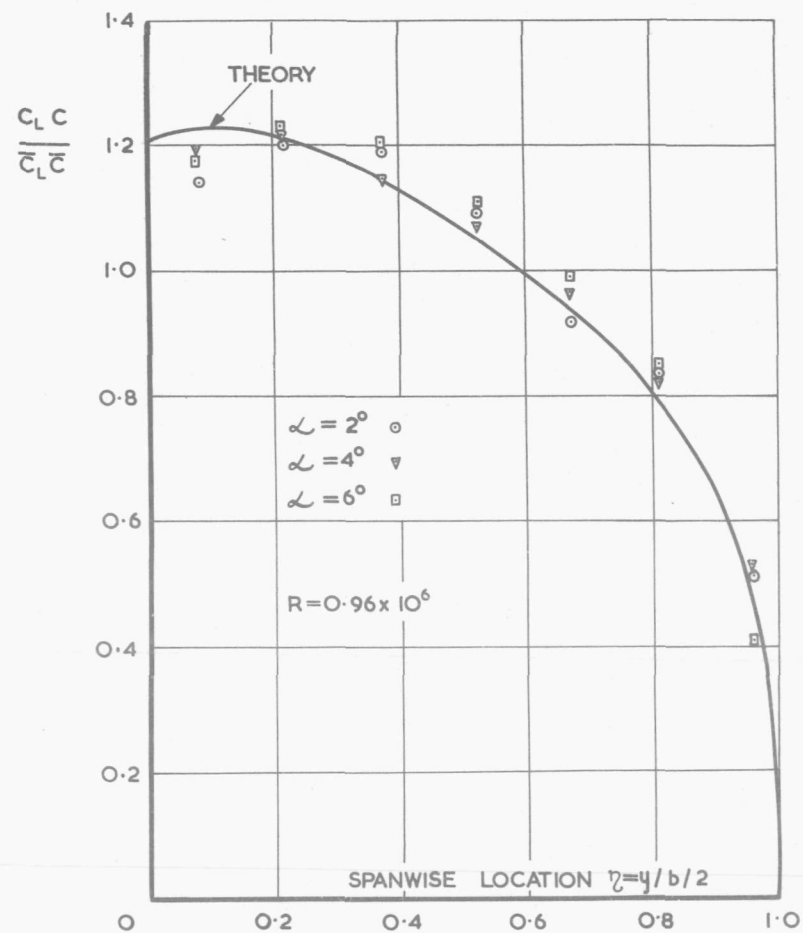
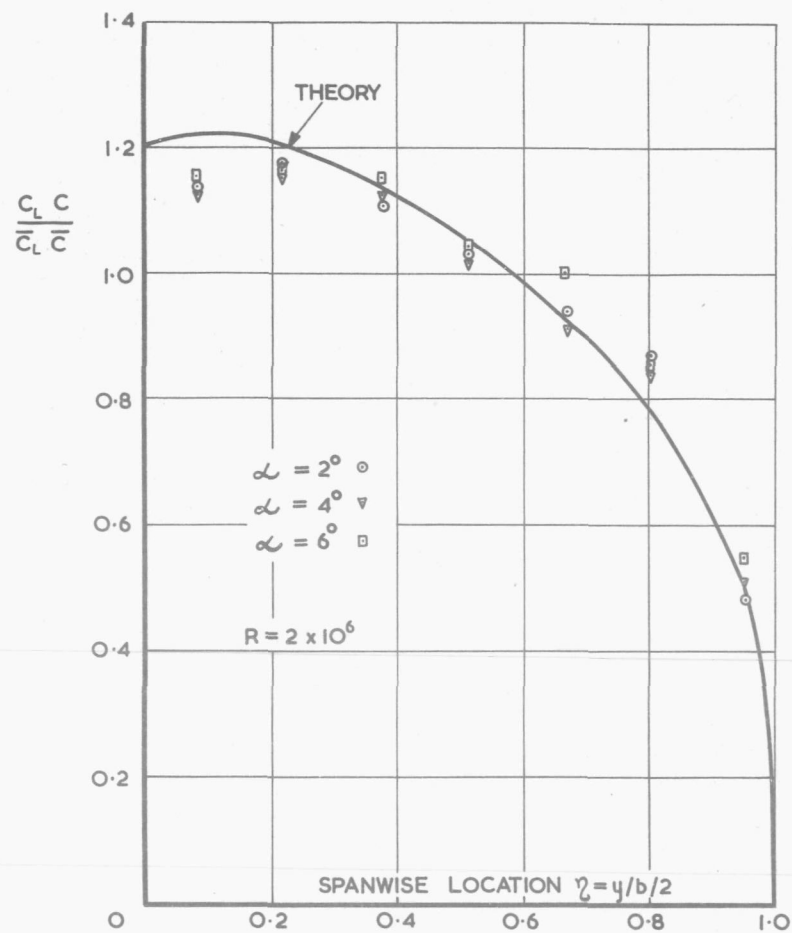


FIG. 7 SPANWISE LOAD DISTRIBUTION

AR=4.5

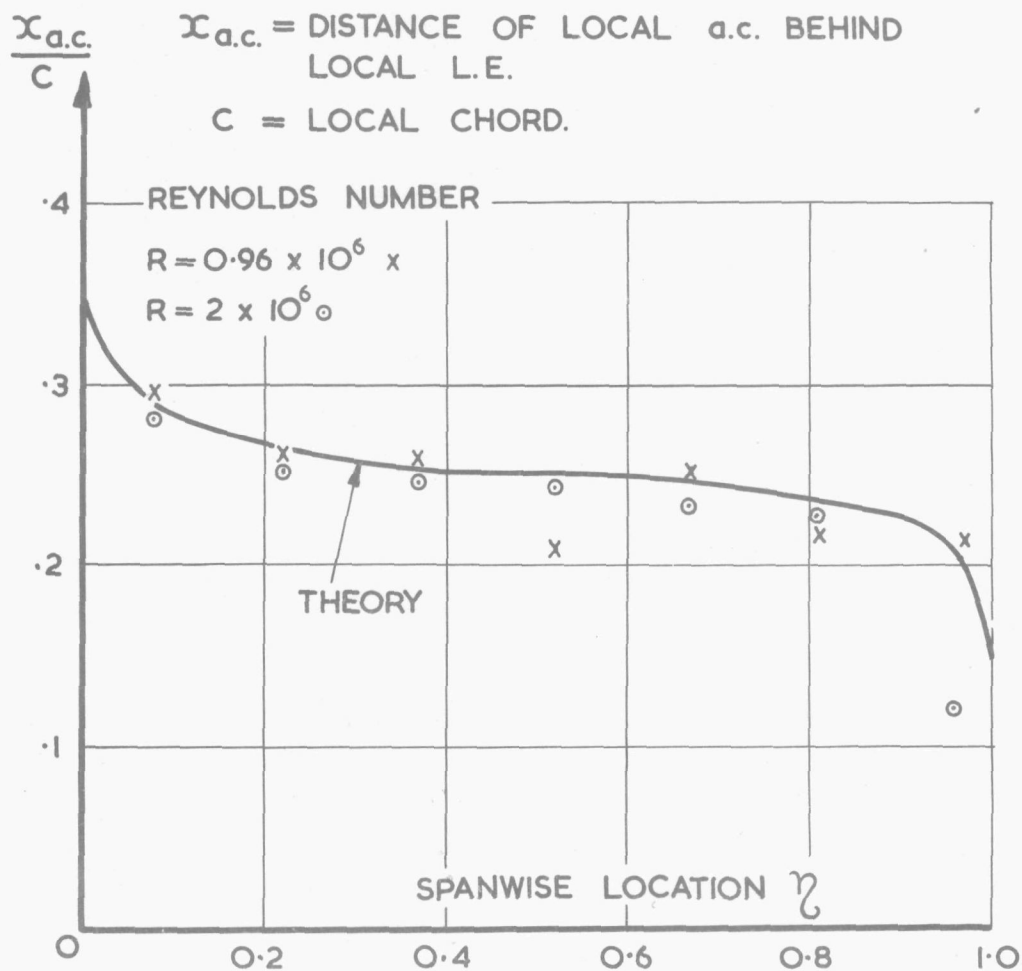


FIG. 8. POSITION OF LOCAL AERODYNAMIC CENTRE ALONG SPAN.